Oxidation kinetics of Si(111) 7×7 in the submonolayer regime

P. Gupta, C. H. Mak, P. A. Coon, and S. M. George
Department of Chemistry, Stanford University, Stanford, California 94305
(Received 3 April 1989; revised manuscript received 12 June 1989)

The kinetics of the initial oxidation of Si(111) 7×7 by O_2 in the submonolayer regime was studied using laser-induced thermal desorption, temperature-programmed desorption, and Auger-electron spectroscopy. The results showed that the oxidation of Si(111) 7×7 by O_2 was characterized by two kinetic processes. Initially, a rapid oxygen uptake step occurred that was followed by a slower growth process which asymptotically approached an apparent saturation oxygen coverage. The initial reactive sticking coefficient (S_0) of O_2 on Si(111) 7×7 decreased with surface temperature from $S_0=0.2$ at 200 K to $S_0=0.06$ at 600 K. The observed decrease in S_0 suggested that the initial oxidation of Si(111) 7×7 was mediated by an O_2 precursor species. In contrast, the apparent saturation oxygen coverage was observed to increase as a function of surface temperature. The apparent saturation oxygen coverage increased from approximately $\Theta=0.4$ ML at 110 K to $\Theta=0.7$ ML at 600 K. Experiments with preadsorbed hydrogen also demonstrated that the initial reactive sticking coefficient for O_2 and the apparent saturation oxygen coverage were reduced as a function of increasing hydrogen coverage on the Si(111) 7×7 surface. This behavior indicated that the oxidation of Si(111) 7×7 requires free dangling-bond sites.

I. INTRODUCTION

The reaction of oxygen with silicon surfaces is of great fundamental and technological interest. Not only is silicon oxidation a model surface reaction, but oxidation also produces dielectric isolation in silicon devices. Understanding this basic reaction becomes increasingly important as integrated circuitry dimensions are reduced to the submicrometer regime. When surface-to-volume ratios are high, the kinetics of silicon surface oxidation may be critical for controlling this essential chemical processing step.

The pioneering work of Deal and Grove[1] has established the kinetics of silicon oxide growth for thicknesses of 300–1000 Å. The kinetics of silicon oxide growth for thicknesses of 15–140 Å has also been investigated.[2,3] In the present work, the oxidation kinetics of Si(111) 7×7 at much smaller coverages in the submonolayer regime are investigated. These experiments complement a similar investigation of the oxidation of Si(100) at submonolayer coverages using different techniques.[4]

In particular, this study focused on the temperature dependence of the two kinetic processes that dictate silicon surface oxidation in the submonolayer regime. Early gas-volumetric measurements[5] have indicated that oxygen adsorption on silicon surfaces is characterized by two distinct processes: a rapid oxygen uptake followed by a slower oxide growth. Fast and slow oxygen adsorption processes have also been observed by numerous other studies on Si(111) 7×7 (Refs. 6–9) and Si(100).[4,6]

This investigation examined the fast step of the two-step adsorption process on Si(111) 7×7 using laser-induced thermal desorption (LITD) techniques to measure the oxidation rate versus surface temperature. These LITD experiments revealed an initial reactive sticking coefficient that decreased as a function of surface temperature. This temperature-dependent sticking coefficient suggested that the initial stage of silicon oxidation is mediated by a weakly adsorbed O_2 precursor species.[4,10–13]

This study also explored the oxidation kinetics of the slow adsorption step on Si(111) 7×7 versus surface temperature using temperature-programmed desorption (TPD) investigations. These TPD experiments disclosed an oxygen uptake rate that decreased versus oxygen coverage and an apparent saturation oxygen coverage that increased versus surface temperature. The reduction of the oxidation rate may be caused by the progressive reduction in the surface reactivity as the adsorbed oxygen ties up surface dangling bonds.[14–16] Likewise, the reduction of the surface oxidation rate and the apparent saturation oxygen coverage may be related to the stress induced by the oxide growth[17–19] or the repulsive electronic effects between electronegative oxygen adatoms.[20] A coverage-dependent activation barrier was employed to explain the reduction of the surface oxidation rates and the apparent saturation oxygen coverages.

In order to explore the nature of the oxygen surface binding sites, this study used LITD and TPD experiments to measure the silicon oxidation kinetics versus preadsorbed hydrogen coverage. These LITD and TPD investigations displayed an initial reactive sticking coefficient and an apparent saturation oxide coverage that both decreased as a function of preadsorbed hydrogen coverage. Because hydrogen is known to tie up dangling bonds on silicon surfaces, these measurements suggested that the oxygen binding sites on Si(111) 7×7 are determined by the availability of surface dangling bonds.

II. EXPERIMENT

A. Vacuum chamber and crystal preparation

The experimental apparatus has previously been described in detail.[21] Briefly, the ultrahigh-vacuum (UHV) chamber was pumped by a 300-l/s ion pump and a titanium sublimation pump (TSP). These pumps maintained background pressures of approximately 4×10^{-10} Torr during these experiments. The chamber could also be pumped by an external liquid-nitrogen-cooled TSP connected to a 50-l/s turbomolecular pump. The chamber was equipped with a low-energy electron diffraction (LEED) spectrometer, a cylindrical mirror analyzer for Auger-electron spectroscopy (AES), and a quadrupole mass spectrometer for LITD and TPD studies.

Single-crystal Si(111) wafers were obtained from Siltec Silicon. These wafers were p-type boron doped with a resistivity of $\rho=1.2\ \Omega$ cm. In addition, the surface of these Si(111) wafers was at an angle of inclination of $\alpha=4°\pm0.5°$ with respect to the Si(111) plane toward the [110] direction. This angle of inclination is typical for device-grade Si(111) wafers used in epitaxial growth processing.

The single-crystal Si(111) wafer was cut using a diamond saw into rectangular samples with dimensions of 1.1×1.0 cm. Individual samples were mounted on a liquid-nitrogen-cooled cryostat on a differentially pumped rotary feedthrough.[22] Sample cooling was achieved by attaching the wafer to a copper support block that was electrically isolated from the cryostat using a 0.035-in.-thick sapphire sheet. The crystal mounting design and technique for sample heating have been described previously.[21]

A W–5 at. % Re/W–26 at. % Re thermocouple was used to measure the temperature of the silicon crystal. The thermocouple was attached to the silicon sample using Ultra-Temp™ 516 ceramic bond manufactured by Aremco Products, Inc. Before attaching the thermocouple, a 0.030-in.-diam hole centered approximately 1.3 mm from the top edge was drilled in the silicon wafer. The thermocouple junction was then positioned in the hole and attached with ceramic adhesive.

The Si(111) surface was cleaned initially in vacuum by slowly annealing the sample to approximately 1350 K. AES peak-to-peak heights for C(*KLL*), O(*KLL*), and Si(*LVV*) were compared after this annealing cycle. Annealing to 1350 K for a period of 2–5 min was then repeated until the [C]/[Si] and [O]/[Si] AES ratios were less than 1×10^{-3}. Samples cleaned in this manner produced sharp 7×7 LEED patterns. Following each oxidation experiment, the crystal was cleaned by flashing to 1150 K.

B. TPD and LITD

Oxygen exposures were achieved by backfilling the UHV chamber with a fixed pressure of oxygen. Temperature-programmed desorption spectra obtained after silicon oxidation experiments were carried out using a linear heating rate of 9 K/s. Due to the instability of the SiO species, the TPD experiments were performed with the crystal placed 5 cm from the front of the ionizer of the mass spectrometer. The only species observed in the TPD spectra was SiO at 950–1050 K.

Laser-induced thermal desorption experiments utilized a TEM-00 Q-switched ruby laser with a temporal width [full width at half maximum (FWHM)] of 80–100 ns and a Gaussian spatial profile.[21] The laser pulses had energies of 2.3 ± 0.1 mJ before entering the chamber. These pulses were focused onto the silicon sample by a 1.0-m lens. The focused laser beam had a Gaussian beam profile at the focus of the lens with a width of 260 μm (FWHM). The laser pulses were directed onto the silicon sample at an angle of approximately 54° with respect to the surface normal. Under such conditions, the desorption spot on the crystal was elliptical. The spot size measured using the spatial autocorrelation method[23] was approximately 420 μm in diameter along the major axis and 250 μm in diameter along the minor axis.

C. Calibration of oxygen coverages

The direct determination of absolute oxygen surface coverage is difficult. No distinct LEED pattern has been observed for oxygen adsorbed on Si(111) 7×7 that could be used to quantify the oxygen coverage.[7] In addition, oxygen uptake by silicon surfaces does not saturate at one monolayer.[8]

Several methods have been used previously to measure the oxygen surface coverage. Oxygen coverages have been estimated in x-ray photoemission spectroscopy (XPS) experiments based on XPS peak areas.[24] AES has also been employed to obtain an approximate measurement of the surface oxygen coverage using Auger peak-to-peak heights corrected for surface sensitivity.[25,26] Unfortunately, these methods are not definitive measures of the oxygen surface coverage.

Absolute oxygen coverages on Si(100) have been determined by calibrating the oxide coverages relative to the oxide coverage deposited by water decomposition.[6] This method has the advantage that the absolute oxide coverage produced by H_2O decomposition can be measured nearly unambiguously. An absolute coverage is obtained because LEED observations on Si(100) have revealed that a saturation exposure of water produces an ordered overlayer of —OH and —H.[27] This ordered overlayer is believed to saturate all the surface dangling bonds[27] and corresponds to an oxygen coverage of $\Theta_O=0.5$ ML, where 1 ML equals one oxygen atom per silicon surface atom.[6]

The oxide coverage calibration procedures used on Si(100) cannot be applied directly to Si(111) 7×7 because H_2O adsorption on Si(111) 7×7 does not produce a well-defined ordered overlayer.[28] Despite the absence of an ordered overlayer, a similar strategy based on H_2 TPD areas can be employed to calibrate the oxygen coverage. For example, previous electron-energy-loss-spectroscopy (EELS) studies of water adsorption on Si(111) 7×7 have shown that H_2O decomposes to yield hydrogen and oxygen dissociation products.[28] TPD experiments have also demonstrated that these dissociation products eventually

will desorb thermally as H_2 and SiO.[29] Thus, relative measures for hydrogen and oxide coverages can be obtained from the integrated areas under the H_2 and SiO TPD peaks.[29]

Two different desorption states designated β_1 and β_2 are observed in H_2 TPD spectra following a saturation exposure of hydrogen.[21,30] The hydrogen coverage following a saturation hydrogen exposure corresponds to 1.0×10^{15} hydrogen atoms/cm^2 on Si(111) 7×7.[31] The high-temperature β_1 state originates from a monohydride species[32] and is saturated at a coverage of 8×10^{14} hydrogen atoms/cm^2.[30] This coverage represents a hydrogen coverage of $\Theta_H=1.0$ ML, where 1 ML corresponds to the number of silicon atoms on the unreconstructed Si(111) surface.

After comparison with the integrated area for a saturated β_1 state following a saturation exposure of hydrogen on Si(111) 7×7, the integrated area under the β_1 state in the H_2 TPD spectra following a water exposure provides an absolute measure of the hydrogen coverage Θ_H. Because of the stoichiometry of water, the absolute oxygen coverage is $\Theta_O=\Theta_H/2$. Consequently, the oxygen Auger signals were calibrated using the absolute oxygen coverages obtained from the β_1-state H_2 TPD measurements after various H_2O exposures. For these oxygen coverage calibrations, the Si(111) 7×7 crystal at 110 K was exposed to various doses of water. The crystal was then annealed to 500 K to desorb the H_2O multilayer. The oxygen Auger calibrations employed I_O/I_{Si}, the [O(*KLL*)]/[Si(*KLL*)] Auger peak-to-peak ratios.

The correlation between the O(*KLL*)/Si(*KLL*) Auger ratio, I_O/I_{Si}, and the absolute oxygen coverages calculated from the β_1-state H_2 TPD peak area was linear. Thus, the absolute oxygen coverages resulting from various O_2 exposures on Si(111) 7×7 could be determined easily using the O(*KLL*)/Si(*KLL*) AES ratios. The area under the SiO TPD spectra at 950–1050 K also provided a relative measure of the surface oxygen coverage. Like the I_O/I_{Si} AES ratios, the SiO TPD areas were observed to be directly proportional to the absolute oxygen coverages.

D. Calibration of LITD signals

The SiO LITD signals must be calibrated before LITD techniques can be used to measure oxidation rates. The SiO LITD signals were calibrated using the following procedure. The Si(111) 7×7 surface was initially exposed to a particular oxygen dose. An AES spectrum was recorded to measure the oxygen coverage. SiO LITD signals were then collected at various surface temperatures. During the collection of the SiO LITD signals, only a very small fraction ($\leq 2\%$) of the total surface oxygen coverage was depleted. Subsequently, a SiO TPD spectrum was recorded in order to provide an additional verification of the surface oxygen coverage after collecting the SiO LITD signals.

The SiO LITD signals measured as a function of oxygen coverage for three surface temperatures T_s are shown in Fig. 1. For all surface temperatures between $T_s=200$ and 600 K, the SiO LITD signals were found to be directly proportional to the oxygen surface coverage. In addition, Fig. 1 shows that the SiO LITD signals were very dependent on the surface temperature. In particular, larger SiO LITD signals were observed for the same surface oxygen coverage at higher surface temperatures.

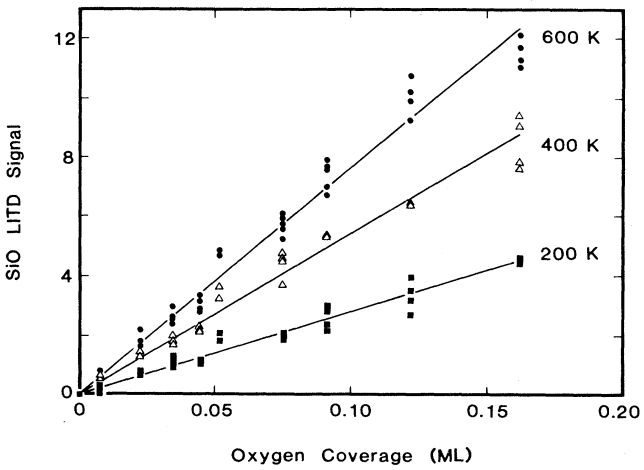

FIG. 1. Laser-induced thermal desorption signals for SiO from Si(111) 7×7 as a function of oxygen coverage at three surface temperatures.

The SiO LITD calibrations described above were performed by summing three consecutive LITD signals for the same desorption spot. For $\Theta_O<0.3$ ML, the combined magnitude of the SiO LITD signals produced by the second and third laser shots was only 10–20 % of the magnitude of the SiO LITD signal from the first laser shot.[33] However, for values of $\Theta_O>0.3$ ML, more than three LITD shots were necessary to deplete the oxygen from the desorption spot. Consequently, the utility of LITD was limited to the study of initial silicon oxidation rates where $\Theta_O<0.3$ ML.

III. RESULTS

A. Initial reactive sticking coefficient

The initial oxidation of Si(111) 7×7 was studied as a function of surface temperature using LITD techniques. In these experiments, the clean Si(111) 7×7 surface was maintained at a constant surface temperature. The surface was then oxidized by backfilling the UHV chamber with a constant pressure of O_2.

During oxidation of the surface, the oxygen coverage on the crystal was measured as a function of time by monitoring the SiO LITD signals. Three consecutive SiO LITD signals were sampled from each surface position in order to deplete the oxygen coverage in that area. After every set of three SiO LITD signals, a new surface position was interrogated. By measuring SiO LITD signals from different positions at different times during O_2 exposure, the oxygen surface coverage was monitored in real time.

The results of the LITD oxidation measurements performed with an O_2 background pressure of 5×10^{-9} Torr for three different surface temperatures are shown in Fig. 2. The initial oxidation rate was proportional to the initial slope of the oxygen uptake curves displayed in Fig. 2. The solid lines shown in Fig. 2 are least-squares fits to the initial slopes of the oxygen uptake curves. Notice that the initial oxidation rate clearly decreases as a function of surface temperature.

Experiments were also performed to check if the presence of hot filaments had any effect on the oxidation rate. These LITD oxidation experiments were performed at an O_2 pressure of 5×10^{-9} Torr and a surface temperature of 600 K with the Auger, ionization gauge, and mass spectrometer filaments off. The surface oxygen coverage was monitored periodically by turning the filaments on briefly for a total of 10 s. During these 10-s periods, five LITD shots were taken to probe the surface oxygen coverage. This procedure was repeated for a total of five times during the course of a 400-s experiment.

The initial oxidation rates obtained from these experiments were consistently within 5–10 % of the results obtained when all the filaments were on continuously throughout the experiment. These results suggest that the presence of hot filaments and "activated oxygen" has a negligible effect on these measurements of the initial oxidation rate of Si(111) 7×7.[34] In contrast, some studies have reported enhanced oxidation caused by ion gauge[7,14,35,36] or Auger[36,37] filaments that were believed to form an excited oxygen species.

Figure 2 also reveals that the oxygen uptake curve is linear only at early time. At a surface temperature of 200 K, the uptake curve starts to deviate from the initial linear behavior when the oxygen coverage reaches approximately $\Theta_O=0.1$ ML. Likewise, the deviation from linearity occurs at later times and higher oxygen coverages for higher surface temperatures. The bending of the oxygen uptake curves indicates that the oxidation rate decreases as a function of increasing oxygen coverage.

The initial oxidation rate was measured at three different O_2 background pressures and various surface temperatures. The initial oxidation rate decreased with increasing surface temperature at each background pressure. In particular, the initial oxidation rate was reduced by approximately a factor of 4 when the surface temperature was raised from 200 to 600 K. The initial oxidation rate was also found to be directly proportional to the O_2 background pressure at a fixed surface temperature. This proportionality indicates that silicon surface oxidation is first order in O_2 pressure.

The initial reactive sticking coefficients S_0 were obtained by dividing the initial oxidation rate by the incident O_2 flux. The incident O_2 flux is simply proportional to the O_2 pressure. The results for the initial reactive sticking coefficient obtained from initial oxidation rates at the three O_2 background pressures are shown in Fig. 3.

Figure 3 reveals that the initial reactive sticking coefficients derived from the oxidation rates at all three O_2 pressures fall on the same curve. As mentioned above, this behavior demonstrates that the initial silicon oxidation rates are first order in oxygen pressure. Likewise, the results in Fig. 3 show that the initial reactive sticking coefficient is temperature dependent. In particular, the initial reactive sticking coefficient decreased from $S_0=0.2$ at 200 K to $S_0=0.06$ at 600 K.

B. Oxygen uptake measurements

The utility of LITD techniques for measuring oxygen coverages was limited to $\Theta_O<0.3$ ML as discussed previously. Consequently, the TPD spectra of SiO were em-

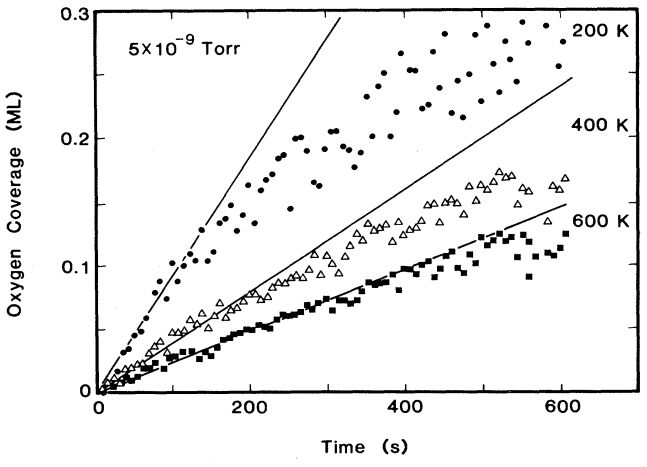

FIG. 2. Initial oxidation of Si(111) 7×7 observed by monitoring the SiO LITD signals vs time at several surface temperatures. The O_2 pressure was 5×10^{-9} Torr. The solid lines are the linear least-squares fits to the initial oxygen uptake curves.

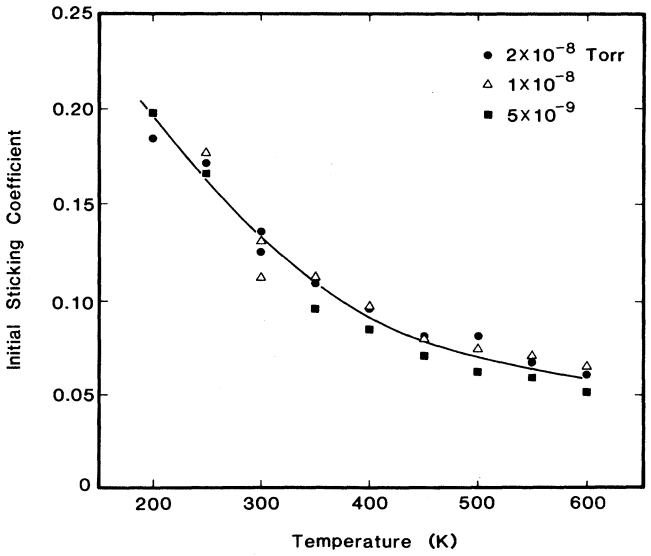

FIG. 3. Initial reactive sticking coefficient for O_2 on Si(111) 7×7 vs surface temperature. The initial sticking coefficients were determined from the initial oxidation rates at three O_2 background pressures.

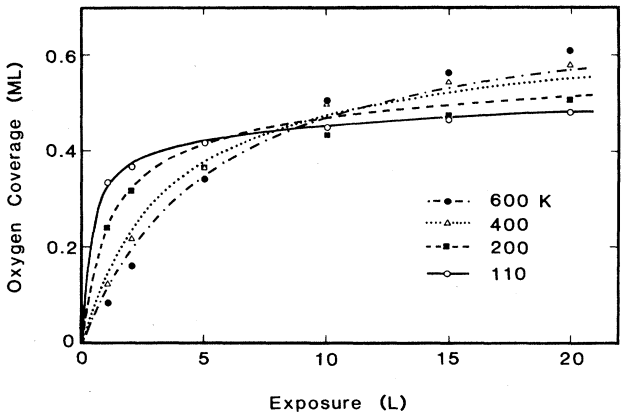

FIG. 4. Oxygen uptake on Si(111) 7×7 vs O_2 exposure at 1×10^{-7} Torr for several surface temperatures. The lines were obtained from the precursor-mediated adsorption model with a coverage-dependent activation barrier, $E_r(\Theta)$.

ployed to study the adsorption of oxygen on Si(111) 7×7 at higher oxygen coverages. The oxygen exposures were performed using an O_2 background pressure of 1×10^{-7} Torr at a variety of surface temperatures from 110 to 600 K. These TPD measurements of oxygen uptake in the low-exposure range are shown by the symbols in Fig. 4. The lines correspond to the model discussed in Sec. IV B for oxygen adsorption with a coverage-dependent activation barrier.

The initial oxidation behavior revealed by the SiO TPD measurements shown in Fig. 4 is similar to the initial oxidation rates determined by the LITD measurements shown in Fig. 2. The oxygen uptake as a function of time is given by the area under the SiO TPD spectra. As before, the slope of the oxygen uptake curves in the limit of zero coverage defines the initial reactive sticking coefficient. Notice that the initial slopes of the oxygen uptake curves clearly decrease with increasing surface temperature.

At intermediate surface oxygen coverages, the silicon oxidation rate decreased dramatically. This decrease leads to a bend in the oxygen uptake curves. This bending occurred at smaller oxygen exposures for lower surface temperatures. In particular, Fig. 4 shows that the oxygen uptake curve at 110 K bends over after an oxygen exposure of 1 L (1 L = 1 langmuir = 10^{-6} Torr s). In contrast, the turnover point occurred at an oxygen exposure of roughly 10 L at a surface temperature of 600 K.

The oxygen uptake curves for higher O_2 exposures are shown in Fig. 5(a). The oxygen exposures larger than 20 L were achieved with an oxygen pressure of 5×10^{-7} Torr. The data points obtained with an O_2 pressure of 1×10^{-7} Torr shown in Fig. 4 are also included in Fig. 5(a). After large O_2 exposures, the oxygen uptake curves appeared to reach a saturation value. However, the apparent saturation oxygen coverage on Si(111) 7×7 was temperature dependent and higher apparent saturation oxygen coverages occurred at higher surface temperatures.

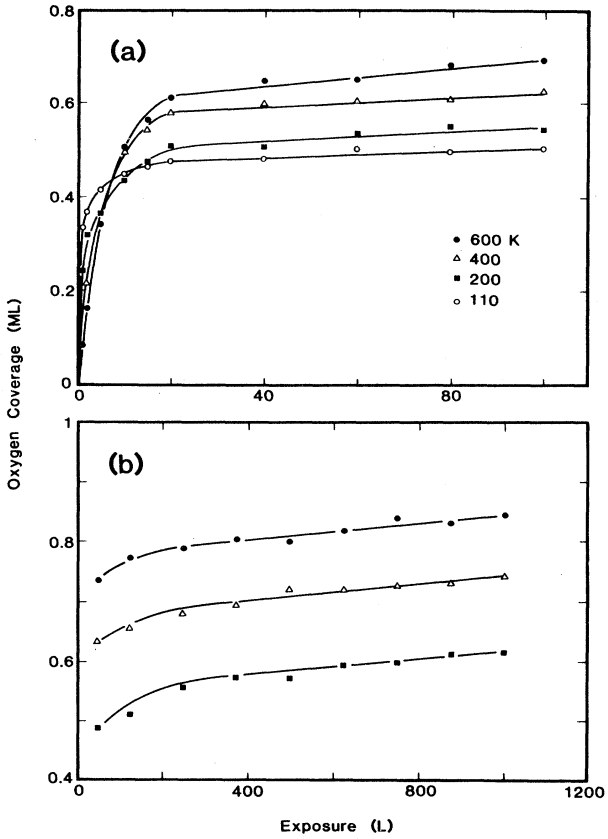

FIG. 5. (a) Oxygen uptake on Si(111) 7×7 vs O_2 exposures up to 100 L for several surface temperatures. (b) Oxygen uptake on Si(111) 7×7 vs O_2 exposures up to 1000 L for several surface temperatures.

Experiments were also conducted to verify if the presence of hot filaments had an effect on the apparent saturation oxygen coverage.[36,38] These oxidation experiments were performed using an O_2 exposure of 20 L and a surface temperature of 110 K with the Auger, ionization gauge, and mass spectrometer filaments and the ion pump off. The oxygen coverages measured using the SiO TPD areas were consistently within 2% of the results obtained when all the filaments and ion pump were on continuously during the experiment.

C. Slow oxidation uptake measurements

Although Fig. 5(a) shows that the oxygen coverage seemed to approach a saturation value asymptotically, the oxygen coverage did not truly saturate even for O_2 exposures up to 1000 L. The oxygen uptake curves for large oxygen exposures from 250 to 1000 L obtained from SiO TPD experiments for three surface temperatures are shown in Fig. 5(b). These exposures were performed with an O_2 pressure of 5×10^{-6} Torr. Notice that the oxygen coverage continued to increase from 250 to 1000 L at all three surface temperatures investigated.

The oxygen uptake curves shown in Fig. 5(b) are roughly linear with O_2 exposure time. Moreover, the ox-

ygen uptake curves for surface temperatures of 200, 400, and 600 K are approximately parallel to each other. Consequently, the oxidation rate of this slow oxidation step was apparently independent of surface temperature for O_2 exposures from 250 to 1000 L. The reactive sticking coefficient in this slow-uptake regime was determined to be approximately $S = 8 \times 10^{-5}$. This reactive sticking coefficient is approximately 3 orders of magnitude smaller than the initial reactive sticking coefficient.

D. Effects of preadsorbed hydrogen

Figure 6 shows the SiO LITD measurements for silicon oxidation at 600 K with an O_2 pressure of 5×10^{-9} Torr for Si(111) 7×7 preadsorbed with various hydrogen coverages. The corresponding measurement for a clean Si(111) 7×7 surface is also displayed for comparison. Figure 6 clearly demonstrates that the initial oxidation rate decreases as a function of increasing hydrogen coverage on Si(111) 7×7.

Results for the initial reactive sticking coefficient for various preadsorbed hydrogen coverages at 200 and 600 K are summarized in Fig. 7. Figure 7 shows that the initial reactive sticking coefficient for O_2 on Si(111) 7×7 decreases in an approximately linear fashion with increasing hydrogen coverage. This behavior suggests that O_2 adsorption on Si(111) 7×7 requires empty dangling-bond sites.

Oxygen uptake curves on Si(111) 7×7 surfaces preadsorbed with various hydrogen coverages were also obtained using SiO TPD measurements. Figure 8 shows the change in the apparent saturation oxygen coverage at 200 K for three preadsorbed hydrogen coverages. In similarity to the results for the initial reactive sticking coefficient, the apparent saturation oxygen coverage also decreased with increasing hydrogen coverage on Si(111) 7×7.

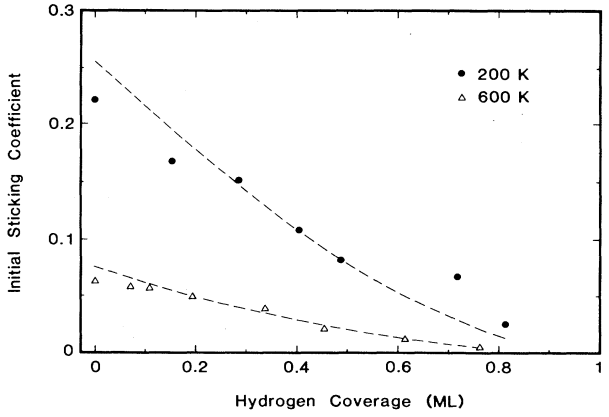

FIG. 7. Initial reactive sticking coefficient of O_2 on Si(111) 7×7 as a function of preadsorbed hydrogen coverage at two surface temperatures. The dashed lines represent the fit of Eq. (4) from the precursor-mediated adsorption model to the initial reactive sticking coefficients.

E. Auger-electron spectroscopy

Auger-electron spectra of the Si(LVV) fine structures between 60 and 90 eV were recorded following different O_2 exposures at various surface temperatures. These Si(LVV) fine structures are sensitive to the chemical environment of the silicon oxide species.[25,39,40] Previous AES studies[25,40] have demonstrated that during the initial stages of silicon oxidation, a new Auger peak develops at 84 eV that is believed to be caused by Si(I) species on the first layer of the surface. The notation Si(I) designates silicon atoms that are bound to only one oxygen atom. Additional Si(II) species induce other AES Si(LVV) peaks at 63 and 70 eV.[35] These Si(II) species result from silicon atoms that are bound to two oxygen atoms that presum-

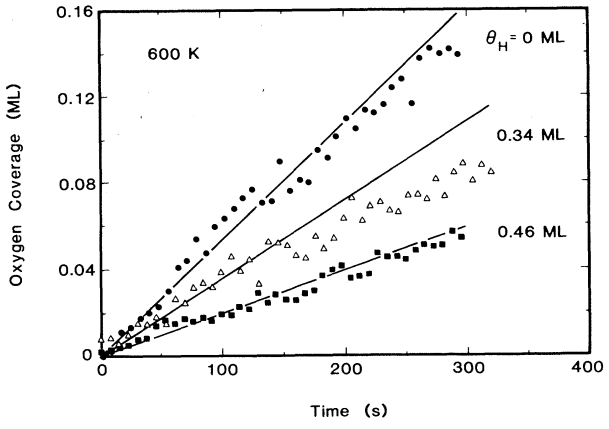

FIG. 6. Effect of preadsorbed hydrogen on the initial oxidation of Si(111) 7×7 at 600 K and an O_2 pressure of 5×10^{-9} Torr. The solid lines are the linear least-squares fits to the initial oxygen uptake curves.

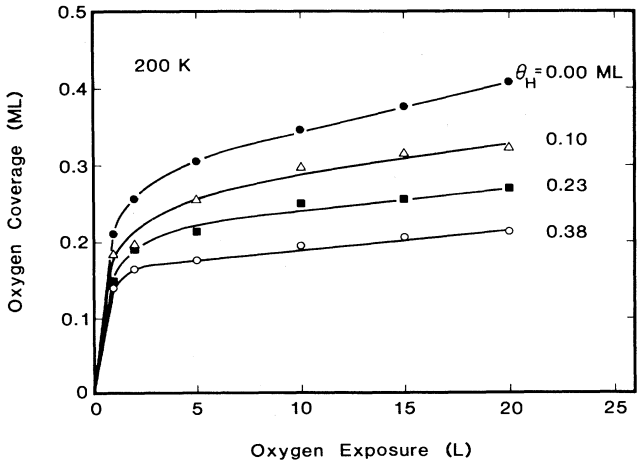

FIG. 8. Effect of preadsorbed hydrogen on the apparent saturation oxygen coverage on Si(111) 7×7 at 200 K.

ably bridge between the first and second layers of silicon atoms on the surface.

The AES spectra of the Si(LVV) fine structures after O_2 exposures of 2, 50, and 1000 L at 200, 400, and 600 K are shown in Fig. 9. These AES spectra were all obtained using the same spectrometer characteristics. However, the AES intensities are not absolute and cannot be compared directly because the silicon sample position could not be duplicated exactly.

After a 2-L O_2 exposure, the negative excursion at 84 eV in Fig. 9(a) appearing as a shoulder on the main AES Si(LVV) peak at 91 eV indicates the presence of the Si(I) species. Additional fine structure at 63 eV also implies that a small amount of Si(II) species have already formed after a 2-L exposure. Because the sticking coefficient decreases with surface temperature, the oxide coverages after the 2-L exposure at 200, 400, and 600 K were approximately $\Theta_O = 0.32$, 0.22, and 0.17 ML, respectively

Figure 9(b) shows the AES spectra obtained after a 50-L O_2 exposure. According to Fig. 5(a), the oxygen coverages have all reached their apparent saturation levels. The AES peaks at 84 eV indicate the presence of Si(I) species. The AES fine structures at 63 and 70 eV also signify that more Si(II) species have formed after a 50-L exposure. Likewise, the nearly equivalent peak shapes for all three temperatures suggest that the relative amounts of the various Si(I) and Si(II) species are similar, even though the total oxygen coverages are different.

After a 1000-L O_2 exposure, Fig. 9(c) illustrates that the features of the AES spectra are quite similar to their counterparts in Fig. 9(b). This similarity suggests that the Si(I) and Si(II) species grow roughly simultaneously from 50 to 1000 L. Figures 9(a)–9(c) also demonstrate that the Auger features are dictated primarily by O_2 exposure and only secondarily by surface temperature.

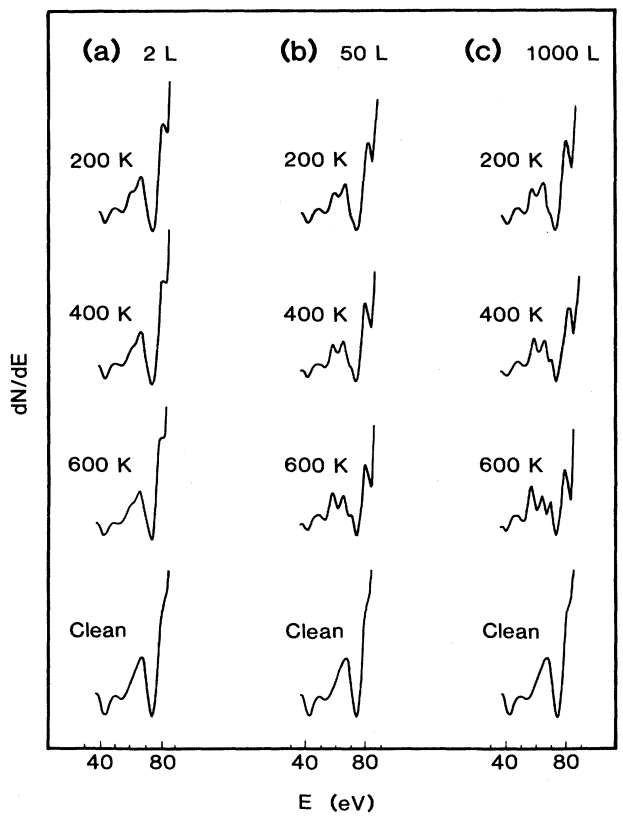

FIG. 9. Si(LVV) AES fine structure for oxygen on Si(111) 7×7 after various O_2 exposures at different surface temperatures.

IV. DISCUSSION

A. Initial reactive sticking coefficients

The initial reactive sticking coefficient of O_2 on silicon surfaces has been the focus of some of the earliest studies of silicon oxidation.[8,9,16,24,34,36,41–46] Previous initial reactive sticking coefficient measurements of O_2 on the Si(111) 7×7 and Si(111) 2×1 surfaces at 300 K are summarized in Table I. The present LITD study measured an O_2 initial reactive sticking coefficient of $S_0 = 0.13$ at 300 K. This result is in very good agreement with previous sticking coefficient measurements of O_2 on Si(111) 7×7.[8,16,24,34,41,45,46]

These initial reactive sticking coefficient measurements were performed using device-grade Si(111) wafers. As is typical for Si(111) wafers used in epitaxial growth processing,[47] the surface of these Si(111) wafers was at an inclination angle of $\alpha = 4°$ with respect to the Si(111) crystallographic plane. However, the annealed Si(111) 7×7 surface with $\alpha = 4°$ does not contain many steps because the steps are known to bunch into facets.[48–50] The excellent agreement between the sticking coefficients measured at 300 K in this study and previous studies summarized in Table I suggests that the step bunches have a negligible effect on the initial reactive sticking coefficient of O_2 on the Si(111) 7×7 surface. A previous study has also observed no difference in the O_2 initial reactive sticking coefficient between a Si(111) 7×7 surface with $\alpha = 0$ and 10°.[34]

TABLE I. Initial reactive sticking coefficient of O_2 on Si(111) 7×7 and Si(111) 2×1 at 300 K.

Surface	S_0	Reference
Si(111) 7×7	0.13	this work
	0.21	41
	0.19	24
	0.18	45
	0.15	8
	0.14	34
	0.10–0.20	16
	0.08	46
	0.01	43
	8×10^{-4}	9
Si(111) 2×1	3×10^{-4}	44
	2×10^{-4}	36
	1×10^{-3}	42
	10^{-3}	16

Previous studies have shown that the initial reactive sticking coefficient of O_2 on the cleaved Si(111) 2×1 surface is 10^2-10^3 lower than for O_2 on Si(111) 7×7.[16,36,42,44,51] Thus, there is a clear difference between the initial reactive sticking coefficient for O_2 on Si(111) 7×7 and the Si(111) 2×1 cleavage surface. Likewise, in contrast to the Si(111) 7×7 investigations, the initial reactive sticking coefficient for Si(111) 2×1 is very dependent on the angle of inclination. The Si(111) 2×1 studies have revealed that the O_2 initial reactive sticking coefficient increases nearly exponentially with angle of inclination α and the surface step concentration.[36,44]

Although the initial reactive sticking coefficient of O_2 on Si(111) 7×7 has been studied extensively at room temperature, the temperature dependence of the initial oxygen sticking coefficient has been measured systematically only on Si(100).[4] Depending on the average translational energy of the O_2 beam, this previous molecular-beam study on Si(100) revealed that the initial reactive sticking coefficient decreased by a factor of between 2 and 10 as temperature increased from 150 to 600 K.[4] Although the absolute values differ, the temperature dependence of the initial reactive sticking coefficient for O_2 on Si(100) with an O_2 translational energy of 2 kcal/mol and the present results are nearly identical.

The initial reactive sticking coefficient for O_2 on Si(111) 7×7 decreased from $S_0=0.2$ at 200 K to $S_0=0.06$ at 600 K. This observed temperature dependence reflects an effective negative activation barrier of -1 kcal/mol. This small activation barrier cannot simply represent the desorption activation energy that would give rise to a temperature-dependent residence time for a physisorbed O_2 species. The physisorption energy for O_2 would be expected to be 4–5 kcal/mol. Consequently, the observed temperature dependence probably reflects the result of two competing activated processes whose activation barriers differ by approximately 1 kcal/mol.

The observed temperature dependence of the initial reactive sticking coefficient is consistent with a precursor-mediated adsorption model.[52,53] In the precursor model, the first stage of adsorption involves the trapping of a precursor species. This precursor species may either dissociate to form chemisorbed oxygen adatoms or desorb into the gas phase. As recently reviewed by Weinberg,[52] this model is represented by the following steps:

$$O_2(g)+nv\xrightarrow{k_a}O_2(\mathrm{ad})\ , \tag{1}$$

$$O_2(g)+nv\xleftarrow{k_d}O_2(\mathrm{ad})\ , \tag{2}$$

$$O_2(\mathrm{ad})+mv\xrightarrow{k_r}2O(\mathrm{ad})\ . \tag{3}$$

In this precursor model, O_2(ad) is the molecular precursor state, O(ad) is the chemisorbed state, and v represents a vacant site. Likewise, k_a is the adsorption rate constant, and k_d and k_r are the desorption and reaction rate constants of the precursor state, respectively. The adsorption rate constant is defined such that $k_a[O_2(g)]=\alpha\phi$, where α is the trapping coefficient of the precursor state and ϕ is the flux of O_2 molecules impinging on the surface.

Using the steady-state approximation for the precursor state, i.e., $(d/dt)[O_2(\mathrm{ad})]=0$, the growth rate of the coverage of the chemisorbed oxygen species, O(ad), is

$$\frac{d\Theta}{dt}=\frac{2\phi\alpha F^{(n+m)}}{F^m+k_d/k_r}\ . \tag{4}$$

In this expression, F represents the fraction of vacant sites. F is employed instead of the concentration of vacant sites, $[v]$, for ease in defining the units correctly. Θ is defined as the coverage of O(ad), the chemisorbed oxygen species. Likewise, the initial reactive sticking coefficient S_0 in the limit $F=1$ is

$$S_0=\lim_{F\to1}\frac{1}{\phi}\frac{d\Theta}{dt}=\frac{\alpha}{1+(k_d^0/k_r^0)\exp[-(E_d-E_r)/RT]}\ . \tag{5}$$

The rate constants k_d and k_r have been expressed in Arrhenius form, where k_d^0 and k_r^0 are the preexponentials and E_d and E_r are the activation barriers.

The parameters in the precursor-mediated adsorption model were determined by fitting Eq. (5) to the results of the LITD measurements for the initial reactive sticking coefficient of O_2 on Si(111) 7×7. The best fits were obtained when $\alpha=0.45$, $k_d^0/k_r^0=15$, and $E_d-E_r=1$ kcal/mol. The solid line in Fig. 3 displays the initial reactive sticking coefficients calculated according to Eq. (5) using these parameters. The agreement between the precursor-mediated adsorption model and the experimental data indicates that the temperature dependence of the initial reactive sticking coefficient for O_2 on Si(111) 7×7 is consistent with the existence of a precursor state.

In the precursor model the precursor state can exist as either a physisorbed or a chemisorbed species.[52] A physisorbed precursor state would be expected to be mobile. Consequently, a physisorbed precursor species should be able to diffuse on the surface and encounter unoccupied sites where the dissociation reaction could take place. However, if adsorption were mediated by this mobile precursor, the sticking coefficient would remain almost constant as a function of increasing coverage. This behavior is not observed for the adsorption of O_2 on Si(111) 7×7. On the contrary, the decrease of the sticking coefficient as a function of oxygen coverage argues against a mobile precursor state. A similar observation for O_2 adsorption on Si(100) is also inconsistent with a mobile physisorbed precursor species.[4]

A precursor state can also exist as a chemisorbed species. Evidence of a possible chemisorbed O_2 precursor species has been provided by EELS,[6,10] XPS,[11,13] and work-function studies.[12] These results have revealed a metastable molecular oxygen species at low surface temperatures that disappears at higher temperatures. This species is generally thought to be either a peroxy radical with only one of the oxygen atoms of the O_2 molecule bonded to a surface dangling bond[6] or a peroxy bridge with both of the oxygens bonded to surface dangling bonds.[11] A fraction of this molecularly chemisorbed

species transforms into more stable silicon oxide species upon thermal annealing.[6,11,13]

B. Apparent saturation oxygen coverage

Figure 5(a) reveals that the apparent saturation oxygen coverage increased as a function of temperature. A similar temperature dependence in the apparent saturation coverage has also been observed for O_2 adsorption on Si(100).[4] Moreover, the apparent saturation oxygen coverage was below one monolayer for all surface temperatures from 110 to 600 K. Previous studies have also reported apparent saturation oxygen coverages below 1 ML for similar surface temperatures.[4,8] The transition between the fast and slow oxidation step occurs at an O_2 exposure of 1–10 L depending on the surface temperature. Previous investigations have also reported similar O_2 exposures that were required to remove the silicon surface states.[7,15]

The adsorption of oxygen on silicon surfaces has been suggested to form compound oxides directly upon adsorption.[4] This hypothesis is supported by XPS (Ref. 7, 15, 54, and 55) and EELS (Refs. 6 and 56) studies that have revealed various SiO_x species of different oxidation states that coexist on the silicon surface even during the early stages of oxidation. With increasing coverage and surface temperature, the distribution of species in the SiO_x mixture shifts to produce higher oxidation states.[7,54,56]

Given the existence of this mixture of SiO_x species on the surface, the adsorption of oxygen on Si(111) 7×7 cannot be described as simple Langmuir adsorption. Likewise, a constant number of adsorption sites does not define the saturation coverage. On the contrary, the TPD oxygen uptake measurements in Fig. 5 demonstrate that the oxygen coverage increases indefinitely with increasing O_2 exposure. The oxygen coverage formed at a given O_2 exposure is also larger at higher surface temperature.

Various mechanisms could explain the temperature-dependent apparent saturation oxygen coverage on Si(111) 7×7. A previous XPS study of oxygen on Si(111) 7×7 (Ref. 7) has indicated that oxygen atoms start to move into the second and third silicon layers at temperatures above 770 K. A more recent XPS and ion-scattering-spectroscopy (ISS) study of oxygen on Si(100) also has suggested that oxygen starts to penetrate the silicon lattice at temperatures between 500 and 700 K.[4] These results would argue that the effective number of oxygen surface binding sites increases with temperature. The temperature dependence of the effective number of binding sites may explain the higher apparent saturation coverages observed at higher temperatures.

The temperature dependence of the apparent saturation oxygen coverage could also be explained if the slow uptake step were an activated process characterized by a coverage-dependent activation barrier, $E_r(\Theta)$. The kinetic process affected by $E_r(\Theta)$ may be the dissociation of the molecular O_2 species given by Eq. (3), the third step in the precursor-mediated adsorption model. A coverage-dependent activation barrier for the O_2 dissociation reaction may result from the stress produced in the silicon surface by oxide growth.[17–19] Because stress increases progressively at higher oxygen coverages, the activation barrier for oxygen incorporation is also likely to increase. The increasing activation barrier would cause the oxygen adsorption rate to decrease as a function of oxygen coverage. Likewise, a temperature-dependent apparent saturation oxygen coverage would be predicted.

Electrostatic effects may also cause the coverage-dependent activation barrier. Adsorbed oxygen atoms have been shown previously to be electron-withdrawing.[20] Consequently, a partial negative charge density accumulates in the near-surface region where the oxygen-silicon bonds are formed. As oxidation proceeds, electrostatic repulsion between oxygen adatoms may cause the activation barrier for oxygen chemisorption to increase as a function of oxygen coverage.

The effects of a coverage-dependent activation barrier on the adsorption of oxygen can be modeled using a coverage-dependent activation barrier in Eq. (3). Based on the kinetics defined by Eqs. (1)–(3), the results of the oxygen uptake measurements in Fig. 4 can be reproduced using the various parameters in the precursor-mediated adsorption model. In these simulations, the activation barrier is given by $E_r(\Theta)=E_r^0+\alpha(\Theta)$. Θ is the oxygen coverage in ML, E_r^0 is the initial activation barrier at zero oxide coverage, and $\alpha(\Theta)$ is the coverage-dependent correction.

Using this coverage-dependent activation barrier, the best fits were obtained with $\alpha(\Theta)=1.5\Theta+\Theta^2+6\Theta^3$ kcal/mol. Both m and n in Eqs. (1)–(3) were chosen to be $m=n=1$. The results of these simulations are shown in Fig. 4. A comparison between the kinetic model and the experimental measurements reveals that the precursor-mediated adsorption model with a coverage-dependent activation barrier for reaction can fit the observed temperature-dependent oxidation of Si(111) 7×7 very closely.

C. Effects of preadsorbed hydrogen

Hydrogen has been shown to tie up dangling bonds on silicon surfaces.[57] Previous UPS and EELS experiments[58] have shown that silicon-monohydride and silicon-dihydride species are formed on hydrogen-covered Si(111) 7×7 surfaces. These silicon-hydride species reduce the dangling-bond density on silicon surfaces. Likewise, reactions with the silicon surface are expected to be inhibited as dangling bonds are passivated by surface hydrogen.[21,32,59]

The decrease in the initial reactive sticking coefficient with preadsorbed hydrogen coverage shown in Fig. 7 argues that the initial adsorption of O_2 on Si(111) 7×7 requires available surface dangling bonds. This conclusion is in accord with the precursor-mediated adsorption model. The precursor-mediated adsorption model hypothesizes that initial silicon oxidation is mediated by a molecularly chemisorbed O_2 precursor species bound to one or two silicon atoms through their dangling bonds. Consequently, a reduction in the dangling bonds caused by the preadsorbed hydrogen atoms would result in a decrease of the initial reactive sticking coefficient.

The effects of reducing the dangling-bond density on

the Si(111) 7×7 surface by preadsorbed hydrogen can be incorporated into the precursor-mediated adsorption model given by Eqs. (1)–(3). Assuming that each preadsorbed hydrogen atom occupies only one dangling bond, the fraction of vacant sites is $F=1-\Theta_H$, where Θ_H is the preadsorbed hydrogen coverage in monolayers. Substituting this expression into Eq. (4) allows the initial reactive sticking coefficient to be calculated as a function of preadsorbed hydrogen coverage Θ_H.

Given that $F=1-\Theta_H$, Eq. (4) was fitted to the initial reactive sticking coefficients at 200 and 600 K versus preadsorbed hydrogen coverage. The best fits were obtained when $\alpha=0.35$, $k_d^0/k_r^0=18$, and $E_d-E_r=1$ kcal/mol. In addition, the values for the constants m and n were assumed to be $m=n=1$. These fits are displayed as the dashed lines in Fig. 7 and they are in good agreement with the experimental data.

In addition to the reduction of the initial reactive sticking coefficient as a function of preadsorbed hydrogen coverage, a similar reduction in the apparent saturation oxygen coverage was observed in Fig. 8. This decrease can also be interpreted as the result of a reduction in the surface dangling-bond density. The dangling bonds occupied by the preadsorbed hydrogen are no longer reactive to oxygen. Consequently, the number of available surface sites for the oxygen reaction decreases and the apparent saturation oxygen coverage is reduced as a function of preadsorbed hydrogen coverage.

D. Oxide species on silicon surfaces

A number of spectroscopic investigations have attempted to elucidate the nature of the oxygen species formed after various stages of silicon oxidation.[6,7,10,11,35,54–56] Several of these studies have revealed various types of adsorbates such as a physisorbed molecular O_2 at 20 K,[10] a peroxy radical at 100 K,[6] and a peroxy species at 150 K.[11] At room temperature and higher temperatures, the various SiO_x species with different silicon oxidation numbers are the main adsorbates on the surface.[7,11,35,54–56] Some studies also speculate that a molecular O_2 species may coexist with the SiO_x species at room temperature.[6,56]

A variety of silicon oxide species appear to be formed even at submonolayer coverages.[7,15] After a 5-L O_2 exposure at 300 K, more than one oxidation state of silicon has been found by the XPS studies.[54] The distribution of SiO_x species with different oxidation numbers does favor the low-oxidation-number species at low oxygen coverages.[7,15,54–56] However, this distribution grows disproportionately at higher coverages and favors the formation of silicon oxides with higher oxidation states.

The AES results in Fig. 9 show a similar behavior. At low coverages, the Si(I) species at 84 eV is the dominant silicon oxide species. The higher oxidation state Si(II) species at 63 and 70 eV develops after longer O_2 exposures, but with the simultaneous growth of the Si(I) species. At higher oxygen coverages, both silicon oxide species grow concomitantly.

The AES results also show an interesting temperature dependence of the oxide formation. At higher surface temperatures, the silicon oxides with higher oxidation state are clearly favored. Figure 9(c) reveals 63- and 70-eV peaks that are much more intense at 600 K compared to the same peaks at 200 K. However, although the distribution of oxidation states shifts to higher oxidation states at higher oxidation temperatures, Fig. 9(c) shows that the AES intensity for the Si(I) species after 1000-L O_2 exposures remains fairly constant as a function of surface temperature. This observation suggests that the oxidation of Si(I) species to produce Si(II) species occurs with approximately equal probability to the oxidation of silicon atoms to produce Si(I) species.

V. CONCLUSIONS

The kinetics of the initial oxidation of Si(111) 7×7 by O_2 in the submonolayer regime has been studied using laser-induced thermal desorption, temperature-programmed desorption, and Auger-electron spectroscopy. The oxidation of Si(111) 7×7 by O_2 was characterized by two kinetic processes: an initial rapid oxygen uptake followed by a slower growth that asymptotically approached an apparent saturation oxygen coverage. The initial reactive sticking coefficient of O_2 on Si(111) 7×7 decreased slowly with surface temperature from $S_0=0.2$ at 200 K to $S_0=0.06$ at 600 K. Using a precursor-mediated adsorption model, the slow decrease in S_0 versus surface temperature was interpreted as the result of competing desorption and reaction pathways.

In contrast to the initial reactive sticking coefficient, the apparent saturation oxygen coverage was observed to increase versus surface temperature. The apparent saturation oxygen coverage increased from approximately $\Theta=0.4$ ML at 110 K to $\Theta=0.7$ ML at 600 K. The temperature dependence of the apparent saturation behavior could be explained by a coverage-dependent activation barrier for the oxidation reaction. This coverage dependence may arise from oxygen-induced surface stress or electrostatic repulsion between oxygen adatoms. Alternatively, oxygen atoms may penetrate into the silicon bulk as a function of temperature and increase the number of free surface sites available for the oxidation reaction.

Experiments with preadsorbed hydrogen demonstrated that the initial reactive sticking coefficient of O_2 was reduced as a function of increasing hydrogen coverage on the Si(111) 7×7 surface. The apparent saturation oxygen coverage also was reduced as a function of preadsorbed hydrogen coverage on Si(111) 7×7. These observations suggested that the adsorption and reaction of O_2 on Si(111) 7×7 requires the availability of surface dangling bonds.

ACKNOWLEDGMENTS

This work was supported by the U.S. Office of Naval Research under Contract No. N00014-86-K-545. Some of the equipment utilized in this work was provided by the National Science Foundation–Materials Research Laboratory (NSF-MRL) program through the Center for Materials Research at Stanford University. One of us (C.H.M.) gratefully acknowledges support from the NSF.

[1]B. E. Deal and A. S. Grove, J. Appl. Phys. **36**, 3770 (1965).
[2]F. P. Fehlner, J. Electrochem. Soc. **119**, 1723 (1972).
[3]A. C. Adams, T. E. Smith, and C. C. Chang, J. Electrochem. Soc. **127**, 1787 (1980).
[4]M. P. D'Evelyn, M. M. Nelson, and T. Engel, Surf. Sci. **186**, 75 (1987).
[5]J. T. Law, J. Phys. Chem. Solids **4**, 91 (1958).
[6]H. Ibach, H. D. Bruchmann, and H. Wagner, Appl. Phys. A **29**, 113 (1982).
[7]M. Tabe, T. T. Chiang, I. Lindau, and W. E. Spicer, Phys. Rev. B **34**, 2706 (1986).
[8]C. A. Carosella and J. Comas, Surf. Sci. **15**, 303 (1969).
[9]B. A. Joyce and J. H. Neave, Surf. Sci. **27**, 499 (1971).
[10]A. J. Schell-Sorokin and J. E. Demuth, Surf. Sci. **157**, 273 (1985).
[11]U. Hofer, P. Morgen, W. Wurth, and E. Umbach, Phys. Rev. Lett. **55**, 2979 (1985).
[12]C. Silvestre and M. Shayegan, J. Vac. Sci. Technol. A **6**, 798 (1988).
[13]U. Hofer, A. Puschmann, D. Coulman, and E. Umbach, Surf. Sci. **211-212**, 948 (1989).
[14]C. M. Garner, I. Lindau, J. N. Miller, P. Pianetta, and W. E. Spicer, J. Vac. Sci. Technol. **14**, 372 (1977).
[15]G. Hollinger and F. J. Himpsel, J. Vac. Sci. Technol. A **1**, 640 (1983).
[16]G. M. Guichar, C. A. Sebenne, G. A. Garry, and M. Balkanski, Surf. Sci. **58**, 374 (1976).
[17]R. J. Jaccodine and W. A. Schlegel, J. Appl. Phys. **37**, 2429 (1966).
[18]J. K. Srivastava and E. A. Irene, J. Electrochem. Soc. **132**, 2815 (1985).
[19]E. Kobeda and E. A. Irene, J. Vac. Sci. Technol. B **5**, 15 (1987).
[20]J. A. Stroscio, R. M. Feenstra, and A. P. Fein, Phys. Rev. Lett. **58**, 1668 (1987).
[21]B. G. Koehler, C. H. Mak, D. A. Arthur, P. A. Coon, and S. M. George, J. Chem. Phys. **89**, 1709 (1988).
[22]S. M. George, J. Vac. Sci. Technol. A **4**, 2394 (1986).
[23]S. M. George, A. M. DeSantolo, and R. B. Hall, Surf. Sci. **159**, L425 (1985).
[24]P. Morgen, W. Wurth, and E. Umbach, Surf. Sci. **152-153**, 1086 (1985).
[25]E. G. Keim, L. Wolterbeek, and A. van Silfhout, Surf. Sci. **180**, 565 (1987).
[26]B. Lang, P. Scholler, and B. Carriere, Surf. Sci. **99**, 103 (1980).
[27]H. Ibach, H. Wagner, and D. Bruchmann, Solid State Commun. **42**, 457 (1982).
[28]M. Nishijima, K. Edamoto, Y. Kubota, S. Tanaka, and M. Onchi, J. Chem. Phys. **84**, 6458 (1986).
[29]B. G. Koehler, C. H. Mak, and S. M. George, Surf. Sci. (to be published).
[30]G. Schulze and M. Henzler, Surf. Sci. **124**, 336 (1983).
[31]R. J. Culbertson, L. C. Feldman, and P. J. Silverman, J. Vac. Sci. Technol. **20**, 868 (1982).
[32]P. Gupta, V. L. Colvin, and S. M. George, Phys. Rev. B **37**, 8234 (1988).
[33]J. L. Brand and S. M. George, Surf. Sci. **167**, 341 (1986).
[34]G. Rovida, E. Zanazzi, and E. Ferroni, Surf. Sci. **14**, 93 (1969).
[35]C. M. Garner, I. Lindau, C. Y. Su, P. Pianetta, and W. E. Spicer, Phys. Rev. B **19**, 3944 (1979).
[36]H. Ibach, K. Horn, R. Dorn, and H. Luth, Surf. Sci. **38**, 433 (1973).
[37]R. E. Kirby and J. W. Dieball, Surf. Sci. **41**, 467 (1974).
[38]M. C. Munoz, V. Martinez, J. A. Tagle, and J. L. Sacedon, J. Phys. C **13**, 4247 (1980).
[39]C. Fiori, Phys. Rev. Lett. **52**, 2077 (1984).
[40]E. G. Keim, Surf. Sci. **148**, L641 (1984).
[41]R. E. Kirby and D. Lichtman, Surf. Sci. **41**, 447 (1974).
[42]R. J. Archer and G. W. Gobeli, J. Phys. Chem. Solids **26**, 343 (1965).
[43]J. Eisinger and J. T. Law, J. Chem. Phys. **30**, 410 (1959).
[44]N. Kasupke and M. Henzler, Surf. Sci. **92**, 407 (1980).
[45]R. E. Schlier and H. E. Farnsworth, J. Chem. Phys. **30**, 917 (1959).
[46]P. E. Wierenga, A. van Silfhout, and M. J. Sparnaay, Surf. Sci. **87**, 43 (1979).
[47]C. W. Pearce, in *VLSI Technology*, edited by S. M. Sze (McGraw-Hill, New York, 1983), Chap. 2.
[48]B. S. Swartzentruber, Y.-W. Mo, M. B. Webb, and M. G. Lagally, J. Vac. Sci. Technol. (to be published).
[49]R. J. Phaneuf, E. D. Williams, and N. C. Bartelt, Phys. Rev. B **38**, 1984 (1988).
[50]E. D. Williams and N. C. Bartelt, Ultramicrosc. (to be published).
[51]C. Y. Yu, P. R. Skeath, I. Lindau, and W. E. Spicer, J. Vac. Sci. Technol. **18**, 843 (1981).
[52]W. H. Weinberg, in *Kinetics of Interface Reactions*, edited by M. Grunze and H. J. Kreuzer (Springer-Verlag, New York, 1987), p. 94.
[53]D. A. King and M. G. Wells, Proc. R. Soc. London, Ser. A **339**, 245 (1974).
[54]G. Hollinger and F. J. Himpsel, Phys. Rev. B **28**, 3651 (1983).
[55]G. Hollinger, J. F. Morar, F. J. Himpsel, G. Hughes, and J. L. Jordan, Surf. Sci. **168**, 609 (1986).
[56]K. Edamoto, Y. Kubota, H. Kobayashi, M. Onchi, and M. Nishijima, J. Chem. Phys. **83**, 428 (1985).
[57]T. Sakurai and H. D. Hagstrum, Phys. Rev. B **12**, 5349 (1975).
[58]R. Butz, E. M. Oellig, H. Ibach, and H. Wagner, Surf. Sci. **147**, 343 (1984).
[59]F. Bozso and Ph. Avouris, Phys. Rev. Lett. **57**, 1185 (1986).